An Deng and Jinrong Feng
Modeling mechanical response of cemented EPS-backfill
Geotechnical Special Publication: Proceedings of the 2013 Congress, 2013; 231:2038-2047

DOI: 10.1061/9780784412787.205

Modeling mechanical response of cemented EPS-backfill

An Deng[1], Jinrong Feng[2]

[1]School of Civil, Environmental and Mining Engineering, IMER, the University of Adelaide, SA, 5034 Australia; an.deng@adelaide.edu.au
[2] Hangzhou Geo-Investigation Design Institute, Hangzhou, Zhejiang, 310000 China; hhuhema@163.com

ABSTRACT: Cemented backfill is one of geomaterials which is used at a high volume to serve a variety of geo-infrastructure systems, e.g., embankments, retaining walls and approach abutments, and involves the solidification of soil or similar fine aggregate through the addition of a controlled amount of cementitious materials, such as Portland cement, fly ash or lime. A certain volume of expanded polystyrene (EPS) pre-puff bead can be incorporated into the backfill matrix to shape the backfill into a mixture, named EPS-backfill, which shows favorable properties a pure backfill rarely exhibits, e.g., reduced unit weight. The ductility of the backfill can also be improved by the inclusion of EPS bead and thus the amendment of material fabric structure. This study was carried out to model the mechanical response of EPS-backfill in terms of the cemented structure of the material. A model was established by treating the shear strength of the material as the combination of bond resistance and friction resistance, which were modeled against elasto-brittle and an elasto-plastic body, respectively. The load share ratio between the two bodies was determined in terms of material breakage undergone by the material. The model was verified against laboratory results of triaxial tests conducted on a series of EPS-backfill samples.

INTRODUCTION

Stability of highway embankment can be increased by reducing the unit weight of backfill, and thus the overburden rested on the soil beneath the embankment. One of the methods to reduce the unit weight is to replace conventional soil backfill with lightweight backfill. There are a variety of lightweight backfills, inclusive of expanded polystyrene (EPS) geofoam, airfoam soil (Watabe et al 2011), soil with rubber chips (Tsoi and Lee 2011), and EPS bead-soil mixture (Onishi et al 2010, Deng and Xiao 2010). The replacement of soil backfill with these lightweight backfills leads to the reduction in unit weight by 20-50%, without comprising the shear or compressive strength and other critical engineering properties of backfill materials. Furthermore, a trend is evolving into a tradition that solid waste materials, e.g., foundry sand, fly ash and dredge slurry, are increasingly being used as the base material in the mixture,

which substantially saves the bottom line of highway embankment construction.

In this study, EPS bead based lightweight material was formed by blending waste foundry sand, fry ash, water and a light amount of Portland cement into a mixture, known as EPS-backfill. To make its use standardized, the backfill was poured in accordance with the specification of controlled low-strength material regulated by American Concrete Institute (ACI) Committee 229 (1999). That is, not only light is EPS-backfill, it also poses the attractions of flowability (for fast construction, self-leveling and compaction), excavability (for future maintenance) and controllable strength (for case-specific purpose). The further benefits of using EPS-backfill as alternative embankment backfill involve its possible capacity of being anti-frost, anti-swelling and anti-vibration. It is expected that EPS-backfill will become one of attractive earth products serving a range of geo-infrastructure systems.

Mechanical response of EPS-backfill plays a vital role in predicting the deformation and progressive failure of the embankment constructed with EPS-backfill when the embankment is subjected to external loads. To depict the mechanical response, a constitutive model was described in this study which was established in terms of the structural characteristics of backfill. A laboratory test was followed to observe the mechanical response of the material, obtain model parameters and verify the model.

DEVELOPMENT OF CONSTITUTIVE MODEL

Characteristics of EPS-Backfill

Cemented EPS-backfill is a solidified continuum. The fabric and structure of the material is substantially altered by the addition of a low amount of cement (Fig. 1), which, for example, may increase the unconfined compressive strength of soil from less than 100 kPa to more than 500 kPa given a cement addition of 50 kg/m^3 (Feng 2009). Cementation may also lead a cemented mixture to a substantial gain of extensile strength, such as 100 kPa on average by a cement addition of 10% (Airey 1993), which granular soils rarely afford. On top of this, EPS-backfill may undergo a unique mode of failure. In light of the schematic fabric of cemented mass shown in Fig. 2, it is indicated that as deformation continues towards failure, cemented particles break apart around contacts, and meanwhile shear resistance gradually comes into effect through the friction resistance generated at particle contacts or interfaces.

The failure mode of EPS-backfill was modeled by introducing two resistances, i.e., bond resistance and friction resistance, as well as the progressive failure or breakage ratio of the material. Before being loaded, EPS-backfill was intact and no breakage took place. At the early stage of loading, the material withstood loads mainly through bond resistance. The friction resistance came into effect only after a definite amount of material deformation and breakage took place, which was often accompanied with strain softening due to the loss of bond resistance (Shen 2006). The loss of bond resistance gradually led to the gain of friction resistance, when the two resistances share loads.

Based on the understandings briefed above, the mechanical response of EPS-backfill was mimicked by a combination of ideal mechanical elements, as did on structural soil by Shen (2006). Three ideal mechanical elements were introduced in this study, i.e., a

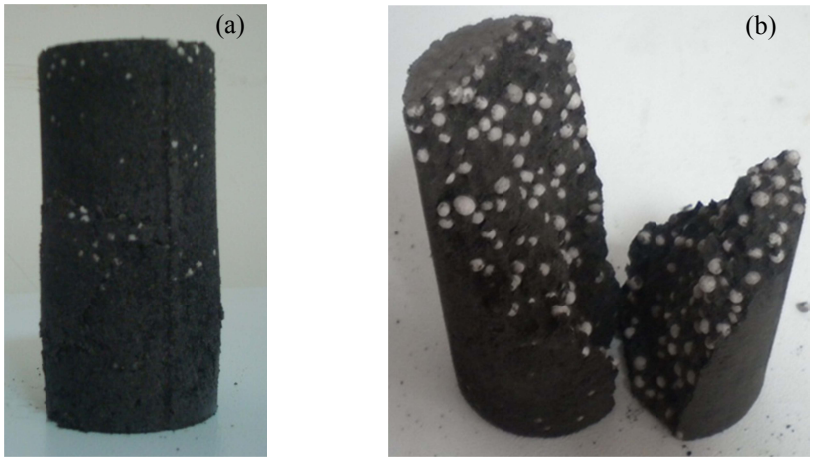

FIG. 1. Cemented EPS-backfill: (a) before shear test, (b) after shear test.

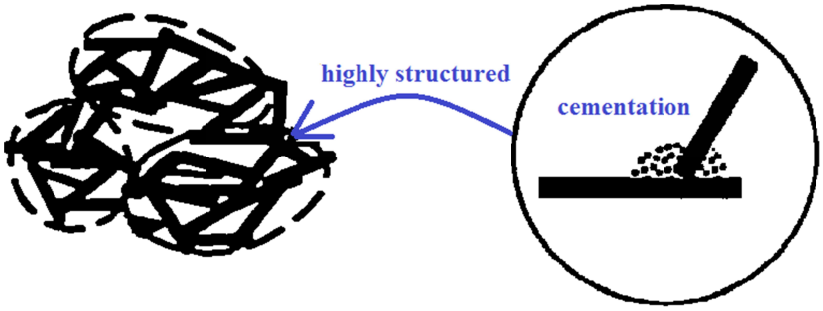

FIG. 2. Schematic fabric of cemented structure.

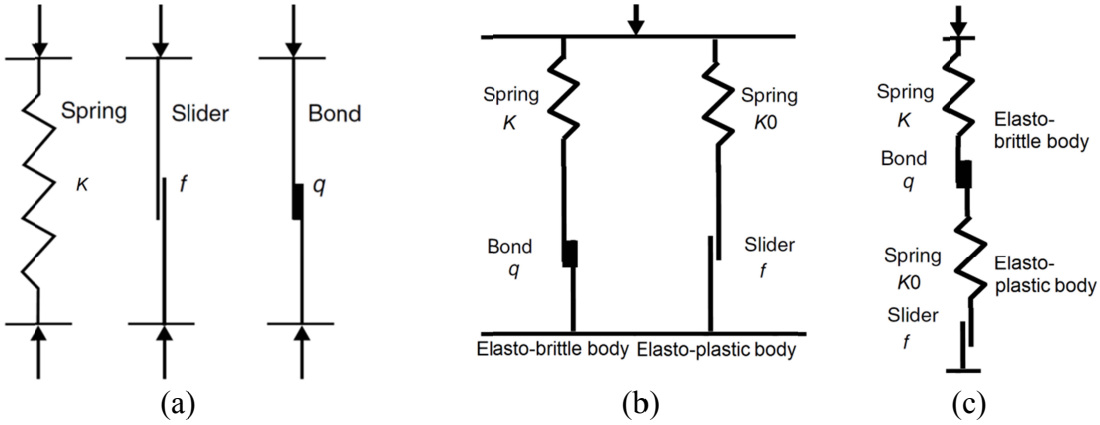

FIG. 3. Schematic diagram of mechanical response: (a) mechanical elements, (b) parallel binary-medium hybrid unit, (c) serial binary-medium hybrid unit.

spring (modulus E), a slider (yield strength f) and a bonded bar (break strength q), as shown in Fig. 3a, corresponding to elastic deformation, plastic yielding and brittle cracking, respectively. Bond resistance was simulated as an elasto-brittle body which combined a spring and a bonded bar, and friction resistance was simulated as an elasto-plastic body which combined a spring and a slider. The trade-off between the

two resistances was calibrated by using a serial, parallel or mixed combination of the two bodies (Fig. 3b-c), which depended on the development of material breakage. The combination led to the establishment of a binary-medium hybrid unit. In relation to unit parameters, the elasto-brittle body was modeled against early-stage elastic behavior of cemented structure, while elasto-plastic body was modeled against an uncemented or reconstituted material.

Establishment of Binary-Medium Hybrid Unit

To depict the load sharing of a binary-medium hybrid unit, homogenization method (Wang et al 2002) was adopted, which splits stress and strain between mechanical bodies in terms of breakage of the materials, as indicated in Eqs. 1-2.

$$\sigma = (1-\xi)\sigma_1 + \xi\sigma_2 \tag{1}$$

$$\varepsilon = (1-\xi)\varepsilon_1 + \xi\varepsilon_2 \tag{2}$$

where, σ and ε are the total stress and strain, respectively, loaded to the hybrid unit, σ_1 and ε_1 are the stress and strain, respectively, shared by elasto-brittle body, σ_2 and ε_2 are the stress and strain, respectively, shared by elasto-plastic body, and ξ is breakage ratio and equals the volume ratio of elasto-plastic body over the unit.

Eqs. 1-2 were rearranged into Eqs. 3-6 by differentiating both sides of the equations and splitting the stress and strain in terms of mean hydrostatic stress (or mean stress), σ_{m}, and deviator shear stress, σ_{s}.

$$\mathrm{d}\sigma_{\mathrm{m}} = \left(1-\xi_{\mathrm{v}}\right)\mathrm{d}\sigma_{\mathrm{m1}} + \xi_{\mathrm{v}}\mathrm{d}\sigma_{\mathrm{m2}} + (\sigma_{\mathrm{m2}} - \sigma_{\mathrm{m1}})\mathrm{d}\xi_{\mathrm{m}} \tag{3}$$

$$\mathrm{d}\sigma_{\mathrm{s}} = \left(1-\xi_{\mathrm{s}}\right)\mathrm{d}\sigma_{\mathrm{s1}} + \xi_{\mathrm{s}}\mathrm{d}\sigma_{\mathrm{s2}} + (\sigma_{\mathrm{s2}} - \sigma_{\mathrm{s1}})\mathrm{d}\xi_{\mathrm{s}} \tag{4}$$

$$\mathrm{d}\varepsilon_{\mathrm{m}} = \left(1-\xi_{\mathrm{m}}\right)\mathrm{d}\varepsilon_{\mathrm{m1}} + \xi_{\mathrm{v}}\mathrm{d}\varepsilon_{\mathrm{m2}} + (\varepsilon_{\mathrm{m2}} - \varepsilon_{\mathrm{m1}})\mathrm{d}\xi_{\mathrm{m}} \tag{5}$$

$$\mathrm{d}\varepsilon_{\mathrm{s}} = \left(1-\xi_{\mathrm{s}}\right)\mathrm{d}\varepsilon_{\mathrm{s1}} + \xi_{\mathrm{s}}\mathrm{d}\varepsilon_{\mathrm{s2}} + (\varepsilon_{\mathrm{s2}} - \varepsilon_{\mathrm{s1}})\mathrm{d}\xi_{\mathrm{s}} \tag{6}$$

where, ξ_{m} is bulk breakage ratio, ξ_{s} is shear breakage ratio, ε_{m} is bulk (volume) strain, ε_{s} is shear strain, σ_{m1} and σ_{m2} are mean stress components shared by elasto-brittle and elasto-plastic bodies, respectively, and linked by bulk load share ratio b_{m} (Eq. 7). Similarly, deviator stress components σ_{s1} and σ_{s2} are linked by shear load share ratio b_{s} (Eq. 8).

$$b_{\mathrm{m}} = \frac{\sigma_{\mathrm{m2}}}{\sigma_{\mathrm{m1}}} \tag{7}$$

$$b_{\mathrm{s}} = \frac{\sigma_{\mathrm{s2}}}{\sigma_{\mathrm{s1}}} \tag{8}$$

It is indicated from Eqs. 5-6 that the bulk strain increment $\mathrm{d}\varepsilon_{\mathrm{m}}$ of a hybrid unit is composed of three components: the bulk strain increment of elasto-brittle body $\mathrm{d}\varepsilon_{\mathrm{m1}}$, the bulk strain increment of elasto-plastic body $\mathrm{d}\varepsilon_{\mathrm{m2}}$ and the bulk strain increment due to cementation bulk breakage $\mathrm{d}\xi_{\mathrm{m}}$. Shear strain increment $\mathrm{d}\varepsilon_{\mathrm{s}}$ comprises of similar three components. The three strain components are described below.

The strain increment of elasto-brittle body can be described in terms of Hooke's law, i.e.,

$$\mathrm{d}\varepsilon_{\mathrm{m1}} = \frac{\mathrm{d}\sigma_{\mathrm{m1}}}{K} \tag{9}$$

$$\mathrm{d}\varepsilon_{\mathrm{s1}} = \frac{\mathrm{d}\sigma_{\mathrm{s1}}}{3G} \tag{10}$$

where, K is bulk modulus, and G is shear modulus.

For the strain increment of elasto-plastic body, classical Modified Cam-clay was

selected to simulate the stress-strain behavior of the elasto-plastic body. The model is able to account for both shear contraction and elasto-plastic behavior of geomaterials, which reflects the shear mode that the elasto-plastic body undergoes. In Modified Cam-clay (Schofield and Wroth 1968), strain increments $\mathrm{d}\varepsilon_{\mathrm{m2}}$ and $\mathrm{d}\varepsilon_{\mathrm{s2}}$ are given in Eqs. 11-12, respectively.

$$\mathrm{d}\varepsilon_{\mathrm{m2}} = \frac{1}{1+e_0}\left[(\lambda-\kappa)\frac{2\eta \mathrm{d}\eta}{M^2+\eta^2} + \lambda\frac{\mathrm{d}\sigma_{\mathrm{m2}}}{\sigma_{\mathrm{m2}}}\right] \tag{11}$$

$$\mathrm{d}\varepsilon_{\mathrm{s2}} = \frac{\lambda-\kappa}{1+e_0}\left[\frac{2\eta}{M^2-\eta^2}\right]\left[\frac{2\eta \mathrm{d}\eta}{M^2+\eta^2} + \frac{\mathrm{d}\sigma_{\mathrm{m2}}}{\sigma_{\mathrm{m2}}}\right] \tag{12}$$

where, $\eta = \sigma_{\mathrm{s2}}/\sigma_{\mathrm{m2}}$, e_0 is initial void ratio, λ and κ are soil constants and equal the average slopes of load and unload-reload lines, respectively, in specific volume-stress (v-ln$p$) plane, and M is a soil constant and equals the aspect ratio of the elliptical yield locus in mean stress-deviator stress (p, q) plane.

For the strain increment due to cementation breakage, breakage ratios ξ_{m} and ξ_{s} vary between 0 and 1 and follow Weibull distribution (Shen 2006). Meanwhile, the ratio ξ_{m} (or ξ_{s}) is associated with material yield bulk stress σ_{m0} (or yield shear stress σ_{s0}) and actual bulk stress σ_{m} (or shear stress σ_{s}), and is presented in Eqs. 13-14, respectively.

$$\xi_{\mathrm{m}} = 1 - e^{-\left(\frac{\sigma_{\mathrm{m}}}{\sigma_{\mathrm{m0}}}\right)^{\mathrm{n}}} \tag{13}$$

$$\xi_{\mathrm{s}} = 1 - e^{-\left(\frac{\sigma_{\mathrm{s}}}{\sigma_{\mathrm{s0}}}\right)^{\mathrm{n}}} \tag{14}$$

where, n is a constant, $\sigma_{\mathrm{m}}=\sigma_{\mathrm{m1}}+\sigma_{\mathrm{m2}}$, and $\sigma_{\mathrm{s}}=\sigma_{\mathrm{s1}}+\sigma_{\mathrm{s2}}$. Differentiating both sides of Eqs. 13-14, we obtain

$$\mathrm{d}\xi_{\mathrm{m}} = e^{-\left(\frac{\sigma_{\mathrm{m}}}{\sigma_{\mathrm{m0}}}\right)^{\mathrm{n}}} \cdot \mathrm{n}\left(\frac{\sigma_{\mathrm{v}}}{\sigma_{\mathrm{v0}}}\right)^{\mathrm{n}-1} \cdot \frac{1}{\sigma_{\mathrm{m0}}}\mathrm{d}\sigma_{\mathrm{m}} \tag{15}$$

$$\mathrm{d}\xi_{\mathrm{s}} = e^{-\left(\frac{\sigma_{\mathrm{s}}}{\sigma_{\mathrm{s0}}}\right)^{\mathrm{n}}} \cdot \mathrm{n}\left(\frac{\sigma_{\mathrm{s}}}{\sigma_{\mathrm{s0}}}\right)^{\mathrm{n}-1} \cdot \frac{1}{\sigma_{\mathrm{s0}}}\mathrm{d}\sigma_{\mathrm{s}} \tag{16}$$

The strain increment of the binary-medium hybrid unit was established in terms of Eqs. 3-16. Four sets of parameters are sought, inclusive of the bulk modulus K and shear modulus G for elasto-brittle body, the initial void ratio e_0, soil constants λ, κ, and M for elasto-plastic body, the yield mean stress σ_{m0} and deviator stress σ_{s0} for breakage, and the bulk load share ratio b_{m} and shear load share ratio b_{s} between the elasto-brittle and elasto-plastic bodies.

For the elasto-brittle body, bulk modulus K approximately equals the initial tangent slope of mean stress-volumetric strain (σ_{m} - ε_{v}) curve obtained from isotropic compression tests. Shear modulus G approximately equals the initial tangent slope of deviator stress-axial deviator strain (σ_{s}-ε_{s}) curve obtained in triaxial compression test.

For the elasto-plastic body, soil constants λ and κ equal the slopes of load and unload-reload lines, respectively, in v-ln$p$ plane obtained from oedometer tests. Constant M equals the slope of failure envelope in stress plane (p, q).

For the breakage, the breakage ratios ξ_{m} and ξ_{s} were obtained from Eqs. 13-14, respectively, in which yield bulk stress σ_{m0} was obtained from isotropic compression tests and yield shear stress σ_{s0} was obtained from triaxial compression tests.

For the bulk load share ratio b_{m} between the elasto-brittle and elasto-plastic bodies, Eq. 17 was used, which was improved in terms of the one (for general soil) suggested by Shen (2006). The improved one is able to maintain a positive b_{m}, while relating the

share ratio to the progressive breakage of EPS-backfill.

$$b_{\mathrm{m}} = \frac{K - K_i}{K - K_0} \tag{17}$$

where, K_0 is the initial bulk modulus of uncemented EPS-backfill (i.e., cement content=0%), and K_i is the bulk modulus of cemented EPS-backfill and equals the bulk modulus of hybrid unit which combines the moduli of elasto-brittle and elasto-plastic bodies.

The combination of elasto-brittle and elasto-plastic bodies is dependent upon the progress of breakage. At the early stage of shear, a parallel unit dominates the mechanical response of EPS-backfill as indicated in Fig. 3(b) where a low amount of breakage takes place and the majority of load is carried by the elasto-brittle body. The combined bulk modulus K_{p} can be estimated by Eq. 18, in terms of the bulk breakage ratio ξ_{m}.

$$K_{\mathrm{p}} = \left(1 - \xi_{\mathrm{m}}\right)K + \xi_{\mathrm{m}}K_0 \tag{18}$$

Along with the increase of shear and extension of breakage, elasto-brittle bodies gradually reach failure criteria and become elasto-plastic, and accordingly are simulated by elasto-plastic bodies. In this stage, the elasto-brittle and elasto-plastic bodies are combined in series, as indicated in Fig. 3(c), the bulk modulus K_{s} of which is estimated by Eq. 19.

$$K_{\mathrm{s}} = \frac{KK_0}{(1-\xi_{\mathrm{m}})K_0 + \xi_{\mathrm{m}}K} \tag{19}$$

To account for the coexistence of the parallel and serial hybrid units, the bulk modulus K_i of the material is equivalent to the combination of K_{p} and K_{s}, and defined in Eq. 20. The definition is associated with bulk breakage ratio ξ_{m}, which is used to quantify the progressive breakage of the material and thus reflect the load share between the parallel and serial hybrid units.

$$K_i = \left(1 - \xi_{\mathrm{m}}\right)K_{\mathrm{p}} + \xi_{\mathrm{m}}K_{\mathrm{s}} \tag{20}$$

Similarly, the shear load share ratio b_{s} between the elasto-brittle and elasto-plastic bodies is presented in Eq. 21.

$$b_{\mathrm{s}} = \frac{G - G_i}{G - G_0} \tag{21}$$

where, G_0 is the initial shear modulus of uncemented EPS-backfill, and G_i is the shear modulus of cemented EPS-backfill, equals the shear modulus of hybrid unit, and defined in Eq. 22.

$$G_i = \left(1 - \xi_{\mathrm{s}}\right)G_{\mathrm{p}} + \xi_{\mathrm{s}}G_{\mathrm{s}} \tag{22}$$

where, G_{p} and G_{s} are defined in Eqs. 23 and 24, respectively.

$$G_{\mathrm{p}} = \left(1 - \xi_{\mathrm{s}}\right)G + \xi_{\mathrm{s}}G_0 \tag{23}$$

$$G_{\mathrm{s}} = \frac{GG_0}{(1-\xi_{\mathrm{s}})K_0 + \xi_{\mathrm{s}}K} \tag{24}$$

LABORATORY TEST AND MODEL VERIFICATION

A laboratory study was carried out to measure the mechanical response of EPS-backfill and verify the model elaborated above. Nine series of EPS-backfill samples were proportioned in accordance with Table 1. Series A1-A5 were made by varying cement content from 0 to 125 kg/m^3, while series B1-B4 were made by varying EPS

bead content from 0 to 6.32 kg/m^3, which aimed to investigate the effects of cement and EPS bead contents, respectively, on mechanical response of EPS-backfill. In fresh state, the samples were produced by complying with the flowability requirement specified for CLSM in ACI R229 (1999). Fresh materials were poured into cylinders (39.1 mm in diameter and 80 mm in height) for further tests after a curing period. From Table 1, it is indicated that the density of EPS-backfill reduces from 1,900 kg/m³ to 923 kg/m³ when EPS content increases from 0 to 6.32 kg/m^3 (equivalently 35% by volume), which evidences the light weight of EPS-backfill.

Table 1. Proportion and Density of EPS-Backfill Samples

Series	Cement (kg/m³)	Fly ash (kg/m³)	Foundry sand (kg/m³)	EPS bead (kg/m³)	Water (kg/m³)	Density (kg/m³)
A1	0	484.0	500	4.21	280	1268.2
A2	50	448.5	500	4.21	280	1282.7
A3	75	430.8	500	4.21	280	1290.0
A4	100	413.0	500	4.21	280	1297.2
A5	125	395.3	500	4.21	280	1304.5
B1	75	430.8	1025	0	370	1900.8
B2	75	430.8	800	2.11	310	1617.9
B3	75	430.8	500	4.21	280	1290.0
B4	75	430.8	135	6.32	276	923.1

The samples were subjected to isotropic compression/swelling and consolidated drained (CD) triaxial compression tests. The samples were cured till day 7 before subjected to both tests. In isotropic compression/swelling, the consolidation loads were applied in sequences of 0, 50, 100, 200, 100, 200, 300 and 400 kPa. Each load was maintained till the volume of a sample barely varied, which lasted about 12 hours. In CD tests, three confinements were used, i.e., 100, 200 and 300 kPa. Axial load was increased at a constant rate of axial strain of 0.015 mm/min or 0.019% strain/min, over which the pore water pressure was controlled below 5% of consolidation pressure. The tests were halted after a peak deviator stress or an apparent failure was reached.

Test results of isotropic compression/swelling are presented in Fig. 4. From Fig. 4(a), it is indicated that cement content plays a major role in affecting the isotropic compression characteristics of EPS-backfill. With the inclusion of cement, the compression curve changes from linear (semi-log scale) style to a convex curve, which may relate to the progressive breakage of cemented structure of the material. That is, cemented backfill underwent a stiffening process in the early stage of isotropic compression, like did on a general soil. Upon approaching the failure strength of cemented structure, breakages took place and specific volume v reduced clearly. Meanwhile, materials were shaped into a hybrid medium, comprising of bonded structure and de-bonded particles. The breakage was progressive and evidenced by the yield trend shown in Fig. 4(a). Along with the increase of cement content, yield stress increases, which means that the more the cement content, the more cohesive the structure, and the higher the load required to fail the bond of the material.

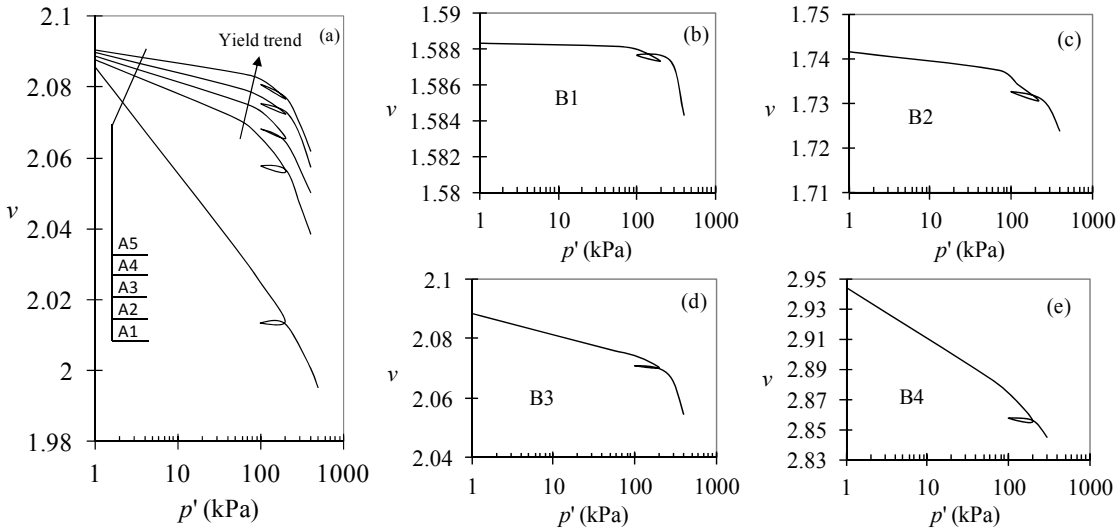

FIG. 4. Isotropic compression and swelling curves: (a) Samples A1-A5 of varying cement content, (b) sample B1 EPS=0, (c) sample B2 EPS=2.11 kg/m^3, (d) sample B3 EPS=4.21 kg/m^3, and (e) sample B4 EPS=6.32 kg/m^3.

Cement content also plays a major role in affecting the unloading (or swelling) characteristics of EPS-backfill. Along with the increase of cement content, the slopes of swelling lines gradually increase, which means that an increasing amount of elastic rebound occurs. That is, the higher the cement content, the more the elastic strain, all other variables maintained the same. This argument is reasonable as high-cement backfill has less volume of breakage (thus less plastic and more elastic strain) than that of low-cement backfill, if the same load is applied.

Figs. 4(b-e) show compression/swelling curves for EPS-backfill samples of varying EPS bead content. Due to the broad variation of specific volume, curves were plotted in individual charts. It is shown that EPS bead content plays a clear effect on the slopes of both loading and unloading lines. The higher the EPS bead, the higher the loading slope, and the lower the unloading slope. That is, the increase of EPS bead content leads to a substantial plastic strain and a marginal elastic strain. It is inferred that EPS bead content should be limited to a certain range, e.g., within 2.11 to 4.21 kg/m^3, if the total volumetric or plastic strain of EPS-backfill is to be controlled.

Fig. 5 shows deviator stress-axial strain curves for selected cemented samples A2, A4 and B2, which were subjected to CD triaxial compression tests. Model results were also plotted against the test results for model verification. Test results of volumetric strain were not correctly collected due to the weak performance of facilities and not presented in the charts. The model parameters were obtained in accordance with the means elaborated in previous section and presented in Table 2.

From Fig. 5, it is indicated that the stress-strain curves of EPS-backfill are strain-hardening, if cement is relatively low and EPS content is relatively high, i.e., sample A2. Otherwise, the curves are strain-softening, i.e., samples A4 and B2. Along with the increase of deviator stress, a linear stress-strain relation is observed at early stage, after which plastic yield takes place when the axial strain of the sample reaches around 4%. Yield strength varies between samples. The higher the confinement, the higher

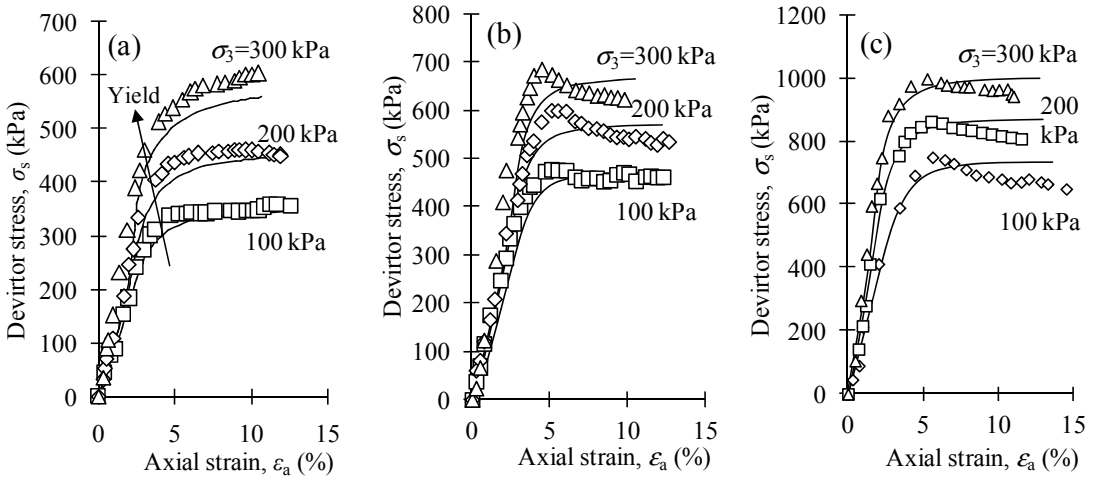

FIG. 5. Test and model results of stress-strain curves from CD compression for samples: (a) A2 (cement=50 kg/m^3 and EPS=4.21 kg/m^3), (b) A4 (cement=100 kg/m^3 and EPS=4.21 kg/m^3), and (c) B2 (cement=75 kg/m^3 and EPS=2.11 kg/m^3).

Table 2. Model Parameters

Series	n	σ_{m0} (kPa)	σ_{s0} (kPa)	K (Mpa)	K_0 (MPa)	G (MPa)	G_0 (MPa)	M	λ	κ	e_0
A2	2	79.6	324.8	6.3	2	3.5	0.79	1.11	0.04	0.003	0.89
A4	2	118.1	430.5	8.4	2	4.8	0.79	1.26	0.03	0.007	0.89
B2	2	187.0	615.0	30.1	2	10.6	0.79	1.38	0.03	0.008	0.54

the yield strength of the material. After deviator stress exceeds individual yield strength, marginal shear strength gains, which means that the majority of bonded structure (elastic-brittle body) was damaged when or just before yielding, and de-bonded mass (elastic-plastic body) withstood minor shear stress.

It is noticed that initial tangent elastic modulus moderately varies between samples of a series. It is interpreted that, at early stage, elastic-brittle body governed the mechanical response of EPS-backfill mass in terms of the hybrid unit aforementioned. Breakage barely took place, nor did the elastic-plastic bodies. As a result, the modulus was significantly associated with elastic-brittle body of the mass, which varied at a marginal scale between samples. The moderate variation was resulted from the difference in confinement (i.e., 100, 200 and 300 kPa) loaded to samples.

It is seen that model results are in good agreement with test results for samples. Three parts of the curves, including the initial linear relation, the yielding and the pre-failure plastic deformation, were modeled at a largely accurate scale, for all three confinements. A minor deficiency of the modeling relates to the weak reflection of strain-softening behavior undergone by samples A4 and B2, which will be amended in next phase modeling work.

On a whole, the binary-medium hybrid unit described in this study is able to model the mechanical response of EPS-backfill at an acceptable level and can be used to predict field deformation when the backfill is placed in a geo-infrastructure system.

CONCLUSIONS

A binary-medium hybrid unit was described to model the mechanical response, in particular, the bonded structure, of cemented EPS-backfill, which is lightweight and used as choice of construction materials for geo-infrastructure systems. The unit treated the mechanical response of EPS-backfill into two components, i.e., bonded structure (elasto-brittle body) and de-bonded particle (elasto-plastic body), which were combined in terms of the breakage (progressive failure) of the material. The hybrid unit was verified against laboratory tests, which, on the other side, were shown to depict the mechanical behavior of the backfill. Stress-strain relation of the backfill is strain-hardening if cement content is low and EPS content is high, or vice versa. Initial tangent moduli moderately vary for a sample subject to different confinements. Yield stress increases along with the increase of cement content and decrease of EPS content. The stress-strain relation is relevant to the cement and EPS contents of the backfill, and the confinement loaded to the material.

ACKNOWLEDGMENTS

The study was originated in Hohai University, continued and completed in the University of Adelaide. The authors appreciate EMCS start-up grant of the University of Adelaide.

REFERENCES

ACI Committee 229 (1999). *Controlled Low Strength Materials* (229R-99). American Concrete Institute, Farmington Hills/MI.

Airey D.W. (1993). "Triaxial testing of naturally cemented carbonate soil." *J. Geotech. Eng*., Vol. 119(9): 1379-1398.

Deng, A. and Xiao Y. (2010). "Measuring and modeling proportion-dependent stress-strain behavior of EPS-sand mixture." *Int. J. Geomech.*, Vol. 10(6): 214-222.

Feng, J.-R. (2009). *Strength and Deformation Behavior of WFS-FA-EPS Based Lightweight Flowable Fill.* A Thesis of Master of Science. Nanjing/Jiangsu.

Onishi, K., Tsukamoto, Y., Saito, R. and Chiyoda, T. (2010). "Strength and small-strain modulus of lightweight geomaterials: Cement-stabilised sand mixed with compressible expanded polystyrene beads." *Geosynth. Int.*, Vol. 17(6): 380-388.

Schofield, A.N. and Wroth, C.P. (1968). *Critical State Soil Mechanics*. McGraw-Hill, London.

Shen, Z.-J. (2006). "Progress in binary medium modeling of geological materials." *Springer Proceedings in Physics: Modern Trends in Geomechanics*, Vol. 106 (Part I): 77-99.

Tsoi, W.Y. and Lee, K.M.. (2010). "Mechanical properties of cemented scrap rubber tyre chips." *Geotechnique*, Vol. 61(2): 133-141

Wang, J.G., Leung, C.F. and Ichicawa, Y. (2002). "A simplified homogenization method for composite soils." *Comp. Geotech.*, Vol. 29(6): 477-500.

Watabe, Y., Saegusa, H., Shinsha, H. and Tsuchida, T. (2011). "Ten year follow-up study of airfoam-treated lightweight soil." *Ground Improv.*, Vol. 164(3): 189-200.